Fourth-order quantum-chromodynamic contributions to the e^+-e^- annihilation cross section

William Celmaster* and Richard J. Gonsalves
Department of Physics, B-019, University of California, San Diego, La Jolla, California 92093
(Received 15 January 1980)

We compute analytically the logarithmic corrections to the photon propagator to order g^4 in massless quantum chromodynamics. With $\alpha_c = g^2/4\pi^2$ defined by momentum-space subtraction, we find that $\sigma(e^+e^- \to \text{hadrons})/\sigma(e^+e^- \to \mu^+\mu^-) = \Sigma_q \epsilon_q^2(1 + \alpha_c + K\alpha_c^2 + \cdots)$, where $K = 463/48 + (85/36\sqrt{3})\mathrm{Cl}_2(\pi/3) - 11\zeta(3) + [(2/3)\zeta(3) - 23/36]n_f = -2.193 + 0.162n_f$ for n_f flavors of quark. The computation is done in momentum space using a novel generalization to $4-\epsilon$ dimensions of the usual Chebyshev-polynomial expansion of Feynman propagators.

I. INTRODUCTION

One of the cleanest and most powerful probes of the short-distance structure of hadrons is the virtual photon produced by annihilation of an energetic pair in colliding beams of electrons and positrons. This process provides a plethora of measurable inclusive cross sections and event shapes that can be used to answer a variety of questions ranging from the existence of new quark species to the form of the fundamental quark-gluon interaction. In this paper we shall be concerned with the total annihilation cross section.

There was early speculation[1] that the total cross section for annihilation to hadrons should behave like const$/E_{\text{c.m.}}^2$ where $E_{\text{c.m.}} = \sqrt{s}$ is the total energy in the c.m. system. Predictions for the constant of proportionality awaited the advent of the parton model,[2] according to which the cross section should be pointlike at high energies and should therefore simply measure the sum of the squares of the electric charges ϵ_i of hadronic constituents.[3] With the discovery of asymptotic freedom,[4] it was realized[5] that the naive parton-model result is an exact prediction of quantum chromodynamics (QCD) at very high energies, and that corrections to this result are calculable in asymptotic perturbation theory

$$\sigma(e^+e^- \to \text{hadrons}) = \frac{4\pi\alpha^2}{3E_{\text{c.m.}}^2}\left(\sum_q \epsilon_q^2\right) \times (1 + \alpha_c + K\alpha_c^2 + \cdots), \quad (1)$$

where[6] $\alpha_c(E_{\text{c.m.}}) = g^2/4\pi^2$ is the QCD running coupling constant and the sum runs over all colors and flavors of quark. That the prediction (1) can be absolutely normalized is a consequence of current conservation. Measurements in the regions above and below the J/ψ resonances have since confirmed the magnitude of this prediction.[7]

That the coefficient of α_c in (1) is exactly 1 was derived[8] soon after the discovery of asymptotic freedom. In this paper we shall present an analytical calculation of the coefficient K of α_c^2. New and more accurate experimental data forthcoming from PETRA and PEP will allow for more stringent tests of these higher-order predictions, and in particular serve to measure α_c in regions between heavy-quark thresholds.

The calculation of K is of interest for several reasons. First, knowing K is necessary from an experimental standpoint because it determines[9] the overall scale of the effective coupling in this process. Thus if we write

$$\alpha_c(Q) = \frac{1}{\beta_0 \ln(Q/\Lambda)} + O\left(\frac{1}{\ln^2(Q/\Lambda)}\right) \quad (2)$$

we see from Eq. (1) that changes in the strong-interaction scale parameter Λ are effects of order α_c^2, and thus Λ cannot be extracted from the data unless K is known to be small.

From a theorist's point of view, the magnitude of K can be used to choose between different definitions of the QCD coupling constant and to estimate the reliability of perturbation theory. There is in fact no universally agreed-upon definition of α_c. Having computed K, one could redefine the expansion parameter in (1) as follows:

$$\alpha_c = \alpha_c'(1 + C\alpha_c' + \cdots), \quad (3)$$

and by suitably choosing C, make the coefficient $K' = K + C$ of $\alpha_c'^2$ as small as one likes. The optimal definition of α_c, however, is one that makes higher-order corrections small in as many different processes as possible. Thus one should compare K with the next-to-leading-order coefficients in deep-inelastic lepton-nucleon[10] and photon-photon scattering,[11] in lepton-pair production,[12] the decay of heavy-quark systems,[13] etc. If there is a definition of α_c which yields small coefficients in several processes, one might hope that its use will minimize higher uncalculated orders of per-

turbation theory in general.

We now give our results for K obtained by using three of the several definitions of α_c that have been suggested in the literature. Using the so-called minimal-subtraction scheme[14] we find that

$$K_{\min} = \tfrac{365}{24} - \tfrac{11}{12} n_f + \frac{\beta_0}{2}[\ln(4\pi) - \gamma_E - 4\zeta(3)]$$

$$= 7.359 - 0.441\, n_f , \qquad (4)$$

where[15] $\beta_0 = \frac{1}{6}(33 - 2n_f)$, $\gamma_E = 0.5772\cdots$ is Euler's constant, $\zeta(3) = \sum_{n=1}^{\infty}(1/n^3) = 1.2021\cdots$, and we have assumed SU(3) of color. We see that $K_{\min}$ is uncomfortably large. Use of minimal subtraction also gives large coefficients in deep-inelastic scattering. In fact, this observation led to the proposal[10] of a modified minimal-subtraction ($\overline{\text{MS}}$) scheme in which the factor[16] $\ln(4\pi) - \gamma_E$ in (4) is absorbed into the definition of α_c. This yields

$$K_{\overline{\text{MS}}} = \tfrac{365}{24} - \tfrac{11}{12} n_f - 2\beta_0\zeta(3) = 1.986 - 0.115\, n_f . \qquad (5)$$

We have proposed[17,18] using momentum-space subtraction to define α_c. Here, all radiative corrections to one of the fundamental vertices of the theory are absorbed into the running coupling constant; one might expect *a priori* that this will yield small higher-order coefficients.[17] The relevant vertex in this problem is the quark-gluon vertex. Upon defining α_c to be the strength of this vertex[19] in the Landau gauge, we obtain

$$K_{\text{mom}} = \frac{463}{48} + \frac{85}{36\sqrt{3}}\,\text{Cl}_2\!\left(\frac{\pi}{2}\right) - \frac{23}{36} n_f - 2\beta_0\zeta(3)$$

$$= -2.193 + 0.162\, n_f , \qquad (6)$$

where

$$\text{Cl}_2(\theta) = \sum_{n=1}^{\infty} \frac{\sin(n\theta)}{n^2}$$

is Clausen's function[20] [$\text{Cl}_2(\pi/3) = 1.014\,942\cdots$]. As shown in Ref. 17, this result is not very sensitive to the choice of the gauge or vertex used to define α_c.

The small values of $K_{\overline{\text{MS}}}$ and K_{mom} show that the definitions of α_c favored by calculations of next-to-leading-order terms in deep-inelastic scattering also yield small coefficients in e^+e^- annihilation. Further comments on the different definitions of α_c and their experimental implications will be relegated to the concluding section.

In Sec. II we review the formalism upon which the calculation is based and straighten out what we have to do to compute K. Section III describes the calculation. In particular, we show how to extend to $N = 4 - \epsilon$ dimensions the usual expansion of a four-dimensional momentum-space propagator in Chebyshev polynomials.[21] Simple formulas are presented which enable one to apply this technique to concrete problems such as the present one. We then analyze the diagrams involved and present the results of the calculation.

II. THE PHOTON PROPAGATOR IN QCD

A. Relating QCD predictions to the data

We work to lowest order in the electrodynamic fine-structure constant α: An electron-positron pair annihilates into a single photon which then turns into a quark-antiquark pair. The subsequent development of the system into the final hadronic state is governed by QCD. The annihilation cross section is given by the discontinuity of the photon propagator

$$\sigma(e^+e^- \to \text{hadrons}) = -\frac{4\pi\alpha}{q^2}\,\text{Im}\,D(-q^2) , \qquad (7)$$

where $q^2 = E_{\text{c.m.}}^2$ and D is defined by the relation

$$\int dx\, e^{iq\cdot x}\langle T A_\mu(x) A_\nu(0)\rangle$$

$$\equiv D_{\mu\nu}(q)$$

$$= \frac{-i}{q^2}\left(g_{\mu\nu} - \frac{q_\mu q_\nu}{q^2}\right) D(-q^2) + \text{gauge term.} \qquad (8)$$

A_μ is the photon-field operator. To avoid possible confusion, we emphasize that (7) holds only in the one-photon approximation; there are other types of contribution to the cross section in higher orders of α. The relation (7) is usually expressed in terms of the spectral amplitude

$$\sum_n (2\pi)^4 \delta^4(p_n - q)\langle 0|J_\mu(0)|n\rangle\langle n|J_\mu(0)|\rangle$$

$$= (q_\mu q_\nu - g_{\mu\nu} q^2)\rho(q^2) \qquad (9)$$

of the hadron electromagnetic-current correlation function as follows

$$\sigma(e^+e^- \to \text{hadrons}) = \frac{8\pi^2\alpha^2}{E_{\text{c.m.}}^2}\,\rho(E_{\text{c.m.}}^2) . \qquad (10)$$

We like to think in terms of the photon propagator (which to order α is simply proportional to the current correlation function) for the following reason: We shall compute $D(-q^2)$ for spacelike q^2 and then continue to the physical region rather than use the direct formula (9) with perturbative quark and gluon intermediate states; D, unlike ρ, has ultraviolet divergences that are not canceled by pure QCD counterterms, and the relation of these divergences to charge renormalization is a little

clearer when one works with the photon propagator rather than the current correlation function.

Strictly speaking, the use of Im $D(-q^2)$ computed in perturbation theory in formula (7) can hardly be justified in spite of the striking agreement of this naive prescription with the data in regions between heavy-quark thresholds. This is equivalent to using perturbative intermediate states in (9) which will inevitably produce threshold singularities for $q^2 > 0$. Relating these singularities to physical hadronic states is essentially a nonperturbative problem. One might hope, however, that the singularities in the perturbative expansion due to thresholds and bound-state formation are smoothed out as one moves away from the real axis. In particular, one should be able to use asymptotic freedom to compute $D(Q^2)$ for large spacelike $q^2 = -Q^2 \ll 0$ and then relate this calculation to the data via a dispersion relation[22]

$$\frac{dD(Q^2)}{d\ln Q^2} = \frac{\alpha Q^2}{3\pi} \int_{4m_\pi^2}^{\infty} \frac{ds R(s)}{(s+Q^2)^2} , \tag{11}$$

where

$$R \equiv \frac{\sigma(e^+e^- \to \text{hadrons})}{\sigma(e^+e^- \to \mu^+\mu^-)} .$$

The rather striking qualitative agreement of the naive prediction $R \approx \sum_q \epsilon_q^2$ based on (1) with the data indicates that one should be able to continue QCD predictions from the spacelike region much closer to the physical region. There have been many proposals as to how this should be done; for example, one of these[23] relates $D(-s-i\Delta)$ to a smeared average of the data

$$\mathrm{Im} D(-s-i\Delta) = -\frac{\alpha\Delta}{3\pi} \int_{4m_\pi^2}^{\infty} \frac{ds' R(s')}{(s'-s)^2+\Delta^2} \tag{12}$$

with $\Delta \approx 3$ GeV^2.

Whether one uses the simple formula (1) or more rigorous relations such as (11) or (12), it is obvious that one cannot neglect the masses of heavy quarks at presently accessible energies. However, quarks with masses $M_i^2 \gg |Q^2|$ effectively decouple from the theory.[24] Between thresholds, the energy dependence of $D(Q^2)$ should be substantially that of the massless theory with the number of quark flavors given by the number of quarks with masses $M_j^2 \ll |Q^2|$. We shall compute the higher-order corrections to $D(Q^2)$ assuming massless quarks. The effects of quark masses to lowest order in α_c have been discussed in Ref. 25.

B. Divergences and renormalization

The function $D(Q^2)$ defined in (8) is dimensionless. Its Q^2 dependence in the massless theory is therefore determined by the divergences of perturbation theory. We shall continue the theory to $N = 4 - \epsilon$ dimensions in order to regulate these divergences which are then manifest as poles in ϵ. In this section we discuss the renormalization of $D(Q^2)$, paying special attention to the dependence of the final result on the definition of the QCD coupling constant.

Let α_B and α_{cB} be the bare electrodynamic and chromodynamic coupling constants, respectively.[6] When computed in perturbation theory, the unrenormalized photon propagator function $D_B(Q)$ takes the form

$$D_B(Q) = 1 + \frac{\alpha_B}{\pi} \sum_{n=1}^{\infty} Q^{-n\epsilon} d_n(\epsilon) \alpha_{cB}{}^{n-1} + O(\alpha_B{}^2). \tag{13}$$

Here $Q = (Q^2)^{1/2}$. The Q dependence follows purely from dimensional analysis: α_B and α_{cB} have dimensions (mass)$^\epsilon$ and Q is the only other dimensionful quantity in the problem. $d_n(\epsilon)$ is the result of computing n-loop Feynman diagrams and is therefore of the form

$$d_n(\epsilon) = \frac{d_{n,n}}{\epsilon^n} + \frac{d_{n,n-1}}{\epsilon^{n-1}} + \cdots + \frac{d_{n,1}}{\epsilon} + d_{n,0} + O(\epsilon), \tag{14}$$

since each loop integration can in general contribute a simple pole.

Now introduce dimensionless renormalized coupling constants α_c and α as follows:

$$\begin{aligned} \alpha_{cB} &= Q_0^\epsilon \alpha_c [1 + (\delta - \beta_0/\epsilon)\alpha_c + O(\alpha_c{}^2)], \\ \alpha_B &= Q_0^\epsilon \alpha [1 + O(\alpha^2)]. \end{aligned} \tag{15}$$

Requiring α and α_c to be dimensionless has forced the introduction of an arbitrary mass scale Q_0 into the theory. $\beta_0 = \frac{1}{6}(11C_{2A} - 2n_f)$ is the well known lowest-order coefficient of the renormalization-group β function.[4,15] δ is a finite constant whose choice leads to different possible definitions of α_c. For α_{cB} fixed, Q_0 and δ are not independent: Rescaling Q_0 amounts to a shift in δ as $\epsilon \to 0$. It is also crucial to note that the radiative corrections in the expansion of α_B in (15) are of order α and not α_c. This is a consequence of the electrodynamic Ward identity which ensures that fermion self-energy and vertex divergences cancel in electric-charge renormalization. We shall see that this implies that $d_{n,n} = 0$ for $n \geq 2$. It has the consequence that the parton-model result $R = \sum_q \epsilon_q^2$ is not multiplicatively renormalized by $(\alpha_c)^{\text{anomalous dimension}}$; the conserved electromagnetic current scales with canonical dimension.

The renormalized photon propagator function is given by

$$D(Q/Q_0, \alpha_c, \alpha) = \lim_{\epsilon \to 0} Z_\gamma^{-1} \times D_B(Q, \alpha_{cB}(Q_0, \alpha_c, \alpha, \epsilon), \alpha_B(Q_0, \alpha_c, \alpha, \epsilon), \epsilon) . \tag{16}$$

Now, strictly speaking, the photon wave-function renormalization constant Z_γ should be chosen such that $D(0, \alpha_c, \alpha) = 1$ in order that α be the standard electrodynamic fine-structure constant with the experimentally measured value 1/137.036. It is obviously impossible to subtract $D_B(Q)$ at $Q = 0$, however, because we have assumed the quarks to be massless. We shall therefore use momentum-space subtraction, i.e., we shall define Z_γ by subtracting D_B at $Q = Q_0$ so that

$$D(1, \alpha_c, \alpha) = 1 . \tag{17}$$

This yields a nonstandard definition of α. For the purposes of this calculation, this is irrelevant since the discrepancy contributes to the total cross section in order α^2. In principle, there should be no difficulty in defining α in the standard fashion because the photon propagator in QCD is not singular at $Q^2 = 0$, the nearest singularity being a branch point at $q^2 = 4m_\pi^2$.

Using the prescription (17) we have

$$D\left(\frac{Q}{Q_0}, \alpha_c, \alpha\right) = \lim_{\epsilon \to 0} \left[1 + \frac{\alpha_B}{\pi} \sum_{n=1}^{\infty} (Q^{-n\epsilon} - Q_0^{-n\epsilon}) d_n(\epsilon) \alpha_{cB}^{n-1} + O(\alpha_B^2)\right] . \tag{18}$$

To perform the summation of dominant powers of $\ln(Q/Q_0)$ for $Q \to \infty$ in (18), one solves the renormalization-group equation gotten by differentiating (18) with respect to Q_0, holding Q, α_B, α_{cB}, and ϵ fixed:

$$\frac{d}{d\ln Q_0} D\left(\frac{Q}{Q_0}, \alpha_c, \alpha\right) = \lim_{\epsilon \to 0} \left[\frac{\alpha_B}{\pi} \sum_{n=1}^{\infty} n\epsilon\, d_n(\epsilon) Q_0^{-n\epsilon} \alpha_{cB}^{n-1} + O(\alpha_B^2)\right] , \equiv \frac{\alpha}{\pi} \Delta(\alpha_c) + O(\alpha^2) , \tag{19}$$

$$\Delta(\alpha_c) = \sum_{n=1}^{\infty} \Delta_n \alpha_c^{n-1} .$$

Using Eqs. (14), (15), and (19) and the fact that the Δ_n are finite in the limit $\epsilon \to 0$, we have

$$\Delta_1 = \lim_{\epsilon \to 0} \epsilon\left(\frac{d_{1,1}}{\epsilon} + d_{1,0}\right) = d_{1,1} ,$$

$$\Delta_2 = \lim_{\epsilon \to 0} 2\epsilon\left(\frac{d_{2,2}}{\epsilon^2} + \frac{d_{2,1}}{\epsilon} + d_{2,0}\right) = 2d_{2,1}, \quad d_{2,2} = 0, \tag{20}$$

$$\Delta_3 = \lim_{\epsilon \to 0} 3\epsilon\left(\frac{d_{3,3}}{\epsilon^3} + \frac{d_{3,2}}{\epsilon^2} + \frac{d_{3,1}}{\epsilon} + \cdots\right) + 2\epsilon\left(\frac{d_{2,1}}{\epsilon} + d_{2,0}\right)\left(\delta - \frac{\beta_0}{\epsilon}\right) = 3d_{3,1} - 2\beta_0 d_{2,0} + 2\delta d_{2,1},$$

$$d_{3,3} = 0, \quad d_{3,2} = \tfrac{2}{3}\beta_0 d_{2,1}$$

In general, all of the residues $d_{n,m}$ for $m > 1$ are determined by the residues $d_{n',1}$ of the simple poles with $n' < n$. It is easy to see that $d_{n,n} = 0$ for $n > 1$. We note that Δ_1 and Δ_2 are uniquely determined while Δ_3 is renormalization-prescription dependent since it involves the constant δ.

Calling $\ln(Q/Q_0) \equiv t$, the solution of (18) with the initial condition (17) is

$$D(e^t, \alpha_c, \alpha) = 1 - \frac{\alpha}{\pi} \int_0^t dt' \Delta(\alpha_c(t')) + O(\alpha^2) , \tag{21}$$

where $\alpha_c(t)$, the invariant charge or running coupling constant, is the solution of the differential equation

$$\frac{d}{dt} \alpha_c(t) = \beta(\alpha_c(t)), \quad \alpha_c(0) = \alpha_c$$
$$\beta(\alpha_c) = -\beta_0 \alpha_c^2 - \beta_1 \alpha_c^3 - \cdots , \tag{22}$$

where[26] $\beta_1 = \frac{1}{12}[17\, C_{2A}^2 - (3C_{2F} + 5C_{2A}) n_f]$. The solution (21) is easily verified using the fact that the invariant charge does not depend on Q_0:

$$\frac{d}{d\ln Q_0} \alpha_c(t) = -\frac{d}{dt} \alpha_c(t) + \frac{d\alpha_c(t)}{d\alpha_c} \frac{d\alpha_c}{d\ln Q_0} = 0 . \tag{23}$$

In the asymptotic region $\alpha_c \ll 1$, Eq. (21) can be integrated using (22)

$$D(e^t, \alpha_c, \alpha) = 1 + \frac{\alpha}{\pi}\left[-t\Delta_1 + \frac{\Delta_2}{\beta_0} \ln\left(\frac{\alpha_c(t)}{\alpha_c}\right) + \left(\frac{\Delta_3}{\beta_0} - \frac{\Delta_2 \beta_1}{\beta_0^2}\right)[\alpha_c(t) - \alpha_c] + \cdots\right] + O(\alpha^2) . \tag{24}$$

The quantity of physical interest is

$$\frac{d}{d\ln Q} D\left(\frac{Q}{Q_0}, \alpha_c, \alpha\right) = -\frac{\alpha}{\pi}[\Delta_1 + \Delta_2 \alpha_c(t) + \Delta_3 \alpha_c^2(t) + \cdots]. \quad (25)$$

Using the naive analytic continuation $Q = e^{-i\pi/2} E_{\text{c.m.}}$ to the physical region and assuming[27] that $\alpha_c \ll \pi/2\beta_0$, we obtain

$$\mathrm{Im} D\left(\frac{Q}{Q_0}, \alpha_c, \alpha\right) = \frac{\alpha}{2}[\Delta_1 + \Delta_2 \alpha_c(|t|) + \Delta_3 \alpha_c^2(|t|) + \cdots], \quad (26)$$

whence $K = \Delta_3/\Delta_1$.

III. THE CALCULATION

A. Feynman diagrams to be computed

The asymptotic behavior of $D(Q)$ is determined by the function Δ. From Eq. (20) we see that the quantities $d_{1,1}$, $d_{2,1}$, $d_{2,0}$, β_0, δ and $d_{3,1}$ determine Δ through order α_c^2.

$d_{1,1}$ is determined by the logarithmically divergent piece of the one-loop diagram in Fig. 1. It was first computed by Schwinger[28] who solved the tricky problem of maintaining gauge invariance. Including a trivial group-theoretic factor we have

$$d_{1,1} = \left(\sum_i \epsilon_i^2\right)\left(-\tfrac{2}{3}\right). \quad (27)$$

The sum is taken over all flavors and colors of quarks.

The residue $d_{2,1}$ of the pole in the diagrams of Fig. 2 is likewise obtainable from the calculation of Jost and Luttinger[29]:

$$d_{2,1} = \left(\sum_i \epsilon_i^2\right)\left(-\frac{C_{2F}}{4}\right). \quad (28)$$

The finite part $d_{2,0}$ of the two-loop diagrams can in principle be extracted from the calculation of the photon propagator through order α^2 in QED (see Kallen and Sabry, Ref. 30) if one allows for the fact that this coefficient depends on how the electron mass is renormalized. In practice, it is not difficult to compute $d_{2,0}$ directly using dimensional regularization; we obtain

$$d_{2,0} = \left(\sum_i \epsilon_i^2\right) C_{2F}\{-\tfrac{55}{48} + \zeta(3) + \tfrac{1}{4}[\gamma_E - \ln(4\pi)]\}. \quad (29)$$

The β-function coefficient β_0 is, of course, well known. The finite renormalization coefficients δ for various renormalization schemes are listed in Table I; these values are taken from Ref. 17 and reproduced here for the convenience of the reader. This leaves the constant $d_{3,1}$ which is the sum of the residues of the simple poles in the diagrams of Fig. 3. A part of $d_{3,1}$ has been computed by Rosner.[31] He obtained the coefficient of $\ln Q$ in the sum of the diagrams in Figs. 3(b) and 3(c) in electrodynamics. This coefficient is, in fact, independent of renormalization prescription and regularization procedure[32] because the electrodynamic Ward identity ensures that all subdivergences cancel. To use Rosner's result we note that the difference between QCD and QED, as far as the diagrams of Figs. 3(b) and 3(c) are concerned, is a trivial multiplicative group-theoretic factor: The QED diagrams corresponding to the uncrossed gluon diagrams of Fig. 3(b) are multiplied by

$$\left(\frac{\pi\alpha_{cB}}{\alpha_B}\right)^2 \left(\sum_i \epsilon_i^2\right)(C_{2F}^2 - C_{2F}C_{2A}/2)$$

to obtain the corresponding QCD results. The pure QCD diagrams of Fig. 3(a) have group-theoretic weight $C_{2F}C_{2A}$ while the diagrams of Fig. 3(d) have weight $C_{2F}n_f$. Thus if we decompose $d_{3,1}$ as follows:

$$d_{3,1} = \left(\sum_i \epsilon_i^2\right) C_{2F}(a_1 C_{2F} + a_2 C_{2A} + a_3 n_f), \quad (30)$$

we see that a_1 is given by Rosner's calculation. To determine a_2 we need to compute the diagrams of Fig. 3(a) and those of either Fig. 3(b) or Fig. 3(c). We choose to compute the diagrams of Fig. 3(b) because diagram D is special in that if requires an extension of the methods developed in this paper as we shall explain later. We find that

$$a_1 = \tfrac{1}{48} \text{ (Rosner)},$$
$$a_2 = \tfrac{11}{6}\zeta(3) - \tfrac{487}{216} + \tfrac{11}{24}(\gamma_E - \ln 4\pi), \quad (31)$$
$$a_3 = -\tfrac{1}{3}\zeta(3) + \tfrac{11}{27} - \tfrac{1}{12}(\gamma_E - \ln 4\pi).$$

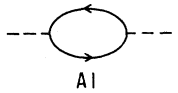

FIG. 1. One-loop diagram whose pole part gives the coefficient $d_{1,1}$. See Eq. (27).

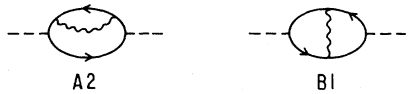

FIG. 2. Second-order QCD corrections to Fig. 1 determine $d_{2,1}$ and $d_{2,0}$. See Eqs. (28) and (29).

TABLE I. Summary of finite renormalization constants δ [see Eq. (15)]. ξ is the covariant gauge parameter: $\xi=0$ for Landau gauge and $\xi=1$ for Feynman gauge. $g=(4/\sqrt{3})\mathrm{Cl}_2(\pi/3)$.

Renormalization scheme		δ
Minimal subtraction (MS) (Ref. 14)		0
$\overline{\mathrm{MS}}$ (Ref. 10)		$\frac{1}{2}\beta_0[\gamma_E-\ln(4\pi)]=\left(\frac{11}{4}-\frac{n_f}{6}\right)[\gamma_E-\ln(4\pi)]\equiv\delta_{\overline{\mathrm{MS}}}$
MS′ (Ref. 16)		$\delta_{\overline{\mathrm{MS}}}-\frac{1}{2}$
Momentum-space subtraction Ref. 17	Three-gluon vertex	$\delta_{\overline{\mathrm{MS}}}-\frac{11}{2}-\frac{23g}{48}+\xi\left(-\frac{9}{16}+\frac{9g}{16}\right)+\xi^2\left(\frac{3}{8}-\frac{g}{8}\right)-\frac{\xi^3}{16}+n_f\left(\frac{1}{3}+\frac{2g}{9}\right)$
	Quark-gluon vertex	$\delta_{\overline{\mathrm{MS}}}-\frac{89}{16}+\frac{85g}{144}+\xi\left(-\frac{25}{24}+\frac{25g}{36}\right)+\xi^2\left(\frac{3}{16}-\frac{g}{16}\right)+\frac{5n_f}{18}$
	Ghost-gluon vertex	$\delta_{\overline{\mathrm{MS}}}-\frac{205}{48}-\frac{5g}{32}+\xi\left(-\frac{9}{8}+\frac{g}{4}\right)+\xi^2\left(-\frac{3}{16}+\frac{g}{32}\right)+\frac{5n_f}{18}$

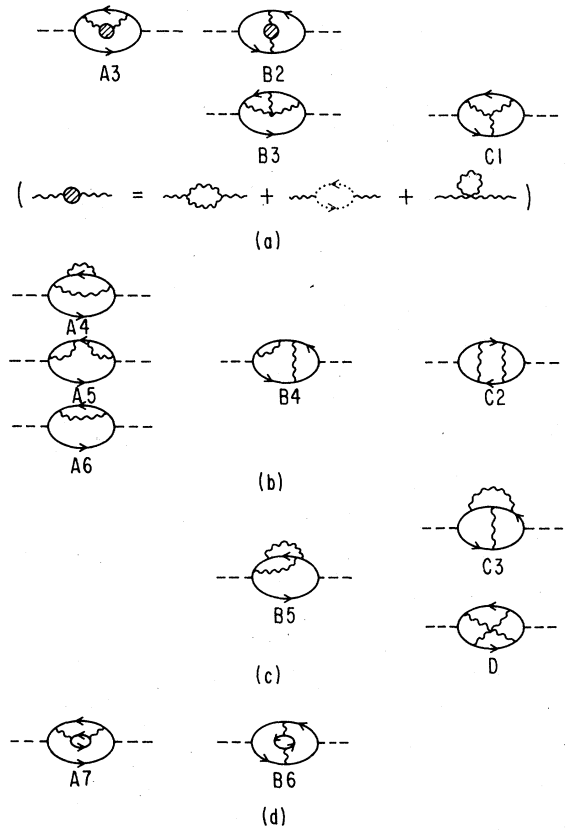

FIG. 3. Diagrams contributing to the vacuum polarization in fourth order. Diagrams in the first, second, and third columns involve essentially one-, two-, and three-loop calculations. Diagrams in (a) are peculiar to QCD while those in (b)–(d) arise also in QED. The simple pole parts of these diagrams determine $d_{3,1}$ in Eq. (30): (b) and (c) contribute to a_1, (a) and (c) to a_2, and (d) to a_3.

B. Gegenbauer expansion in $4-\epsilon$ dimensions

To compute the Feynman diagrams of Figs. 2 and 3 we will use a generalization of the well known[21] Chebyshev-polynomial expansion of propagator denominators to $4-\epsilon$ dimensions working directly in momentum space. This expansion is very different from the position-space formalism that has recently been suggested,[33] but it is just as practical and easy to work with as our calculation will demonstrate. In this section we will present the general formulas involved in a form suitable for practical application.

Consider the denominator

$$(\vec{k}-\vec{l})^2=k^2+l^2-2kl\,\hat{k}\cdot\hat{l} \tag{32}$$

of the propagator of a massless particle with momentum $\vec{k}-\vec{l}$. $\vec{k}$ and $\vec{l}$ are vectors in N-dimensional Euclidean space; $k\equiv(\vec{k}^2)^{1/2}$ and $\hat{k}\cdot\hat{l}$ is the cosine of the angle between $\vec{k}$ and $\vec{l}$. Since the Gegenbauer polynomials[34] $C_n^\lambda(\hat{k}\cdot\hat{l})$, $n=0,1,2,\ldots$, $\lambda>-\frac{1}{2}$ form a complete set on the interval $(-1,1)$, an expansion of the type

$$\frac{1}{(\vec{k}-\vec{l})^2}=\sum_{n=0}^{\infty} f_n(k,l)C_n^\lambda(\hat{k}\cdot\hat{l}) \tag{33}$$

can be made. The C_n^λ can be generated from $C_0^\lambda\equiv 1$ using the following recursion formula[34]:

$$2(n+\lambda)tC_n^\lambda(t)=(n+1)C_{n+1}^\lambda(t)+(1-\delta_{n,0})(n+2\lambda-1)C_{n-1}^\lambda(t)\ . \tag{34}$$

Familiar special cases of these polynomials are the Legendre polynomials ($\lambda=\frac{1}{2}$) and the Chebyshev polynomials ($\lambda=1$) which have useful orthogonality

properties in 3 and 4 dimensions, respectively. We shall choose the index λ so that the C_n^λ are orthogonal on the N-dimensional sphere. From the orthogonality relation[34]

$$\int_{-\pi}^{+\pi} d\theta(\sin\theta)^{2\lambda} C_n^\lambda(\cos\theta) C_m^\lambda(\cos\theta) = \delta_{n,m} \frac{\pi 2^{1-2\lambda}\Gamma(n+2\lambda)}{n!(n+\lambda)[\Gamma(\lambda)]^2}, \quad (35)$$

it follows that if we choose $\lambda = \frac{1}{2}N - 1 = 1 - \epsilon/2$, then

$$\frac{1}{\Omega_N}\int d_N\hat{k}\, C_n^\lambda(\hat{k}\cdot\hat{l}) C_m^\lambda(\hat{k}\cdot\hat{l}) = A_n \delta_{n,m}, \qquad A_n = \frac{\lambda\Gamma(n+2\lambda)}{n!(n+\lambda)\Gamma(2\lambda)}, \quad (36)$$

where

$$d_N\vec{k} \equiv k^{N-1}dk\, d_N\hat{k}, \qquad \int d_N\hat{k} \equiv \frac{2\pi^{N/2}}{\Gamma(N/2)} \equiv \Omega_N. \quad (37)$$

Equation (36) is most easily derived from Eq. (35) by choosing the z axis in the direction $\hat{l}$ in analogy with spherical polar coordinates in 3 dimensions; one then has

$$\int d_N\hat{k} = \int d_{N-1}\hat{k} \int_{-\pi}^{\pi} [\sin(\hat{k}\cdot\hat{l})]^{N-2} d(\cos^{-1}\hat{k}\cdot\hat{l}).$$

Using the addition theorem[34]

$$C_n^\lambda(\cos\phi_1\cos\theta_1 + \sin\phi_1\sin\theta_1\cos\theta_2) = \frac{\Gamma(2\lambda-1)}{[\Gamma(\lambda)]^2}\sum_{m=0}^{n} 4^m \frac{\Gamma(n-m+1)[\Gamma(\lambda+m)]^2}{\Gamma(n+m+2\lambda)} \times (2m+2\lambda-1)(\sin\phi_1\sin\theta_1)^m C_{n-m}^{\lambda+m}(\cos\phi_1) C_{n-m}^{\lambda+m}(\cos\theta_1) C_m^{\lambda-1/2}(\cos\theta_2) \quad (38)$$

for Gegenbauer polynomials, one obtains the very useful convolution formula

$$\frac{1}{\Omega_N}\int d_N\hat{k}\, C_n^\lambda(\hat{k}\cdot\hat{l}) C_m^\lambda(\hat{k}\cdot\hat{q}) = \delta_{n,m} B_n C_n^\lambda(\hat{l}\cdot\hat{q}), \quad (39)$$

$$B_n = \frac{\lambda}{n+\lambda}.$$

This formula is easily derived by choosing a coordinate system such that $\hat{l} = (1, \vec{0}_{N-1})$, $\hat{q} = (\cos\phi_1, \sin\phi_1, \vec{0}_{N-2})$, $k = (\cos\theta_1, \sin\theta_1\cos\theta_2, \hat{k}_{N-2})$ and

$$\int d_N\hat{k} = \int d_{N-2}\hat{k} \int_{-\pi}^{\pi} (\sin\theta_2)^{N-3} d\theta_2 \int_{-\pi}^{\pi} (\sin\theta_1)^{N-2} d\theta_1.$$

It turns out that the formulas (34), (36), and (39) suffice to perform all the angular integrations we shall encounter in this problem.

It remains to specify the functions $f_n(k, l)$ in Eq. (33). They are, in fact, related to the Gegenbauer functions of the second kind $D_n^\lambda(z)$ which are the solutions of the differential equation

$$\left[(z^2-1)\frac{d^2}{dz^2} + (2n+1)z\frac{d}{dz} - n(n+2\lambda)\right] D_n^\lambda(z) = 0 \quad (40)$$

that are irregular at the singular points $z = \pm 1$. [The Gegenbauer polynomials are the regular solutions of Eq. (40).] The relation can be derived from the expansion[35]

$$\frac{1}{z-t} = e^{-i\pi\lambda} 2^{2\lambda}[\Gamma(\lambda)]^2 (z^2-1)^{\lambda-1/2} \times \sum_{n=0}^{\infty} \frac{(n+\lambda)\Gamma(n+1)}{\Gamma(n+2\lambda)} C_n^\lambda(t) D_n^\lambda(z). \quad (41)$$

For our purposes it is more convenient to express the $f_n(k, l)$ in terms of hypergeometric functions whose properties are better known. Using Eq. (41) and the relation[35]

$$D_n^\lambda(z) = e^{i\pi\lambda}[z + (z^2-1)^{1/2}]^{-n-2\lambda} \frac{\Gamma(n+2\lambda)}{\Gamma(\lambda)\Gamma(n+\lambda+1)} \times {}_2F_1\left(\lambda, n+2\lambda;\ n+\lambda+1;\ \frac{z-(z^2-1)^{1/2}}{z+(z^2-1)^{1/2}}\right), \quad (42)$$

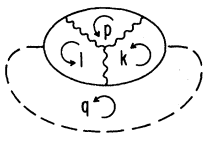

FIG. 4. The "Mercedes-Benz" diagram C1 showing a "planar" choice of momentum routings. The external momentum q is held fixed. It is easily seen that each propagator involves at most two momenta.

we obtain

$$f_n(k,l)=\frac{1}{(kl)_>}\, z_{kl}{}^n G_n(z_{kl}{}^2)\ ,$$

$$(kl)_>=\begin{cases}k^2, & \text{if } k>l,\\ l^2, & \text{if } l>k,\end{cases}$$

$$z_{kl}=\begin{cases}\dfrac{l}{k}, & \text{if } k>l,\\ \dfrac{k}{l}, & \text{if } l>k,\end{cases} \tag{43}$$

$$G_n(x)=\frac{\Gamma(\lambda)\Gamma(n+1)}{\Gamma(n+\lambda)}(1-x)^{2\lambda-1}$$

$$\times\ {}_2F_1(\lambda,\, n+2\lambda;\ n+\lambda+1;\ x)\ ,$$

where the hypergeometric function ${}_2F_1$ has the series expansion

$${}_2F_1(a,b;c;x)=\sum_{n=0}^{\infty}\frac{(a)_n(b)_n}{(c)_n}\frac{x^n}{n!}\ ,$$

$$(a)_0=1, \tag{44}$$

$$(a)_n=a(a+1)(a+2)\cdots(a+n-1),\quad n>1\ .$$

We note that for $N=4$ (i.e., $\lambda=1$), $G_n=1$ and we recover the standard Chebyshev expansion of the propagator.

In practice, one only needs the first few terms in an expansion of G_n in powers of ϵ. Thus in the present calculation, we have found it sufficient to know

(i) $G_n(0)$ to order ϵ^2 for $n\leq 3$,

(ii) $\dfrac{d}{dx}G_n(x)\big|_{x=0}$ to order ϵ^2 for $n\leq 1$,

(iii) $G_n(x)$ to order ϵ for $n\leq 3$.

The derivatives of $G_n(x)$ at $x=0$ can be written down immediately for arbitrary ϵ using the formula

$$\frac{d^m}{dx^m}\ {}_2F_1(a,b;c;x)\Big|_{x=0}=\frac{(a)_m(b)_m}{(c)_m}\ .$$

With a little more effort (see Appendix A), one obtains the following very simple formula for the complete x dependence of G_n through order ϵ:

$$G_n(x)=1+\frac{\epsilon}{2}\left[(1-\delta_{n,0})\sum_{j=1}^{n}\left(\frac{1}{j}\right)\right.$$

$$\left.+(n+1)\sum_{j=1}^{\infty}\frac{x^j}{j\,(n+j+1)}\right]+O(\epsilon^2)\ . \tag{45}$$

In order to estimate the convergence of various radial integrals encountered in this calculation, it is sufficient to know (see Appendix A) that $G_n(x)$ is analytic for $|x|<1$ and that for $x\to 1$,

$$G_n(x)=(n+\lambda)\left[\frac{\Gamma(2\lambda-1)\Gamma(n+1)}{\Gamma(n+2\lambda)}+\frac{\Gamma(\lambda)\Gamma(1-2\lambda)}{\Gamma(1-\lambda)}(1-x)^{1-\epsilon}+O\big((1-x)^{2-\epsilon}\big)\right]. \tag{46}$$

In order to compute a diagram such as Fig. 3(a) B2, it is useful to have an expansion for $[(\vec{k}-\vec{l})^{-2}]^{1+\epsilon/2}$ which is the behavior of a one-loop corrected propagator carrying momentum $\vec{k}-\vec{l}$ in the massless theory; such an expansion is worked out in Appendix A.

As an example of the use of these formulas, we evaluate the quadratically divergent integral

$$\int d_N\vec{k}\,\frac{1}{(\vec{k}-\vec{q})^2}=\int_0^{\infty}k^{3-\epsilon}\,dk\int d_N\hat{k}\,\frac{1}{(kq)_>}\sum_{n=0}^{\infty}z_{kq}{}^n\,G_n(z_{kq}{}^2)C_n^{\lambda}(\hat{k}\cdot\hat{q})$$

$$=\Omega_N A_0\int_0^{\infty}k^{3-\epsilon}\,dk\,\frac{G_0(z_{kq}{}^2)}{(kq)_>}\ . \tag{47}$$

We have used the orthogonality relation (36) to evaluate the angular integral. The radial integral splits into two parts corresponding to $q>k$ and $q<k$:

$$\int_0^{\infty}dk\,\frac{k^{3-\epsilon}}{(kq)_>}G_0(z_{kq}{}^2)=\int_0^{q}dk\,\frac{k^{3-\epsilon}}{q^2}\,G_0\!\left(\frac{k^2}{q^2}\right)+\int_q^{\infty}dk\,\frac{k^{3-\epsilon}}{k^2}\,G_0\!\left(\frac{q^2}{k^2}\right)$$

$$=q^{2-\epsilon}\left[\int_0^1 dY\,Y^{3-\epsilon}G_0(Y^2)+\int_0^1 dX\,X^{-3+\epsilon}G_0(X^2)\right], \tag{48}$$

where we have let $k = qY$ in the first integral and $k = q/X$ in the second. Since $G_0(z) \sim \text{const}$ as $z \to 1$ for $\epsilon \approx 0$, the Y integral is convergent and can be evaluated at $\epsilon = 0$. The X integral converges at the lower limit $X = 0$ (i.e., $k = \infty$) only if $\epsilon > 2$. However, if we make the analytic continuation to $\epsilon > 2$, the integral (47) becomes infrared divergent at $k = q$ (i.e., $X = Y = 1$); indeed, $G_0(z) \sim (1-z)^{1-\epsilon}$ for $\epsilon > 2$. It is in fact well known[36] that the integral (47) cannot be evaluated consistently by naive dimensional continuation. This integral is therefore set equal to zero by fiat—a regularization prescription that is consistent with the Ward identities. Within the Gegenbauer expansion formalism, this prescription can be implemented by using the following rule: Assume that $0 < \epsilon < 1$ and simply discard the divergent contribution at the $k = \infty$ limit of integration [i.e., at $X = 0$ in Eq. (48), for example]. Thus, if $\epsilon < 1$ we can use the expansion (45) in Eq. (48) to obtain

$$q^{2-\epsilon}\left[\int_0^1 dY\, Y^3 + \int_0^1 dX\, X^{-3+\epsilon}\left(1+\frac{\epsilon X^2}{4}\right)+O(\epsilon)\right]$$

$$= q^{2-\epsilon}\left[\frac{1}{4}+\left(\frac{1}{-2+\epsilon}+\frac{\epsilon}{4}\,\frac{1}{\epsilon}\right)+O(\epsilon)\right]$$

$$= O(\epsilon)\,. \tag{49}$$

It can be shown that this prescription sets the quadratically divergent integral (47) to zero to all orders in ϵ.

The diagrams in Figs. 1, 2, and 3 are all potentially quadratically divergent, although, of course, gauge invariance requires that these divergences cancel among themselves. In the present calculation, these divergences will all be manifest as simple one-dimensional integrals such as the X integral in Eq. (48); we use the prescription given above, namely discard contributions at $X = 0$ to regulate these divergences consistently throughout the calculation.

C. Application of the Gegenbauer-expansion technique

Our calculational technique has three novel aspects when compared with previous calculations of the vacuum polarization.[21, 28, 29] First, we use the Gegenbauer expansion of propagator denominators described in the previous subsection working directly in momentum space and in $4-\epsilon$ dimensions. This formalism we believe is new. Second, we use the external momentum as an infrared cutoff and so we never have to introduce a mass into any propagator to regulate infrared divergences. Third, the spurious quadratic divergences that were the bane of previous calculations of the vacuum polarization are, as shown in the previous subsection, trivial to deal with when one uses dimensional regularization. Accordingly, we find we can compute $D(Q)$ directly rather than having to differentiate with respect to Q in order to eliminate the quadratic divergences.

To simplify numerators as much as possible we use the transversality of the photon propagator [see Eq. (8)]:

$$D_B(Q) = \frac{-i}{(3-\epsilon)q^2}\left[\frac{g^{\mu\nu}D_{\mu\nu,B}(q)}{(-i/q^2)^2}\right]. \tag{50}$$

The factor in brackets receives contributions from the diagrams of Figs. 1, 2, and 3, with the external lines amputated and the polarization indices μ and ν contracted together.[37] Since the electrodynamic current is conserved and a color singlet, $D(Q)$ is invariant under general color-gauge transformations. Dimensional regularization respects this gauge invariance. We choose to do the calculation in the Feynman gauge.

In order to use the Gegenbauer-expansion formalism, it must be possible to choose loop momenta and a routing of the external momentum through the diagram such that every propagator denominator has one of two forms: k_i^2 or $(\vec{k}_i - \vec{k}_j)^2$, where $\{\vec{k}_i\}$ is the set consisting of the loop momenta and the external momentum. It is easy to see that it is always possible to do so if the diagram gotten by joining together the two external photon lines is topologically planar.[38] All the diagrams of Figs. 1, 2, and 3, with the exception of Fig. 3(c)D satisfy this criterion. As an example, Fig. 4 shows a "planar" choice of momentum routings for the "Mercedes-Benz" diagram and makes the above assertion about planarity intuitively obvious. The corresponding Feynman integral is

$$\int \frac{d_N\vec{k}\, d_N\vec{l}\, d_N\vec{p}\,(\text{numerator trace})}{k^2 l^2 p^2(\vec{k}-\vec{l})^2(\vec{k}-\vec{p})^2(\vec{l}-\vec{p})^2(\vec{k}-\vec{q})^2(\vec{l}-\vec{q})^2}\,. \tag{51}$$

The five denominators which involve differences of two momenta can be expanded in Gegenbauer polynomials. Because the Lorentz indices of the photon have been contracted, the numerator is a polynomial in the dot products of $\vec{k}$, $\vec{l}$, $\vec{p}$, and $\vec{q}$. The direction cosines in the numerator can be reduced to Gegenbauer polynomials using Eq. (34). Thus the seemingly complicated integral (51) is, in principle, not more complicated than the simple one-loop example discussed in the previous subsection: The angular integrands are products of Gegenbauer polynomials and the radial integrands are polynomials in k, l, and p. In prac-

tice, the integrals are difficult to compute simply because of the large number of terms involved; for example, the numerator trace in (51) consists of 133 terms.

There are a few technical details which are best discussed by dividing the diagrams into four classes.

Class A: Diagrams A1, A2, A3, A4, A5, A6, and A7. It is obvious that these diagrams can be viewed as a succession of one-loop propagator insertions in one-loop propagator diagrams. They are therefore completely trivial to compute in the massless theory.

Class B: Diagrams B1, B2, B3, B4, B5, and B6. Diagram B1 is really a two-loop diagram because the one-loop vertex insertion is sufficiently complicated that it is of no great advantage to compute it first and then insert the result in the one-loop diagram of Fig. 1. Diagrams B2, B4, and B6 are essentially two-loop diagrams with one-loop propagator insertions in one of the internal lines. Now, since the bare coupling constant α_{cB} has dimensions $(\text{mass})^{\epsilon}$, a one-loop gluon-propagator insertion is necessarily of the form

$$-\frac{i}{k^2}\left(g_{\mu\nu}-\frac{k_\mu k_\nu}{k^2}\right)\frac{\alpha_{cB}}{k^{\epsilon}}\left(\frac{a}{\epsilon}+b+c\epsilon+\cdots\right), \tag{52}$$

while a dressed quark propagator is of the form

$$\frac{i\not{k}}{k^2}\,\frac{\alpha_{cB}}{k^{\epsilon}}\left(\frac{a'}{\epsilon}+b'+c'\epsilon+\cdots\right). \tag{53}$$

The transversality of the gluon propagator follows from gauge invariance, and the electrodynamic Ward identity further allows us to drop the $k_\mu k_\nu$ term in (52) when it is inserted, for example, into the sum of diagrams B1 and A2. In diagram B4 one can choose momentum routings so that the dressed quark propagator carries a single momentum variable. In diagrams B2 and B6 by contrast, the dressed gluon must carry two momenta for any "planar" routing of variables. In order to treat the dressed gluon as an insertion in a two-loop diagram, one needs the expansion of a denominator of the form $[1/(\vec{k}-\vec{l})^2]^{1+\epsilon/2}$. In Appendix A we use a simple trick to derive such an expansion. Diagrams B3 and B5 are best treated by computing the two-loop quark-propagator insertions first; these are of the form

$$\frac{i\not{k}}{k^2}\,\frac{\alpha_{cB}{}^2}{k^{2\epsilon}}\left(\frac{a''}{\epsilon^2}+\frac{b''}{\epsilon}+c''+\cdots\right). \tag{54}$$

The remaining one-loop calculation is trivial.

Thus the diagrams of class B essentially involve the calculation of two-loop diagrams through order[39] ϵ^0. Each of these diagrams has three propagator denominators which must be expanded in Gegenbauer polynomials. The two angular integrations reduce the three infinite series so obtained to one. The radial integrations are then straightforward. The $1/\epsilon^2$ and $1/\epsilon$ pieces of the two-loop diagrams arise only from the first few terms of this series; being integrals of simple powers of momenta, the residues are rational numbers. The terms of order ϵ^0 can involve an infinite series of the form

$$\sum_{n=1}^{\infty}\frac{1}{(n+a)(n+b)(n+c)}, \tag{55}$$

with a, b, and c positive integers. Using a partial-fraction decomposition, these sums can be expressed in terms of the transcendental numbers $\zeta(2)=\sum_{n=1}^{\infty}1/n^2=\pi^2/6$ and $\zeta(3)=\sum_{n=1}^{\infty}1/n^3$. The remarkable fact is that if one factors $\Omega_N{}^2=[2\pi^{N/2}/\Gamma(N/2)]^2$ out of these two-loop diagrams then the residuum is free of $\zeta(2)$. In fact, the same is true of all the three-loop diagrams: The pole part of any of the Feynman integrals divided by $\Omega_N{}^3(\alpha_B/\pi)\alpha_{cB}{}^2$ is free of the transcendental numbers π, γ_E, and $\zeta(2)$ which appear in various intermediate stages of the calculation—it is given entirely in terms of rational numbers and the one transcendental number[40] $\zeta(3)$.

The numerators of the two-loop parts of class B diagrams involve typically on the order of ten terms. Each of these is a propagator diagram involving three momenta, two loop and one external, which can be ordered in 3! different ways. Thus there are six regions of integration in the radial variables, but symmetry considerations can usually be invoked to reduce this number to three. Diagrams B1, B2, and B6 were computed by hand. Nevertheless, this calculation was of sufficient complexity that it was decided to use the computer program MACSYMA to compute all the diagrams of this class. It was found that all of these diagrams could be reduced to the calculation of 28 integrals. Appendix B contains a table of these integrals.

Class C: Diagrams C1, C2, and C3. These are essentially three-loop calculations. We need only the pole parts of these diagrams: It turns out that ϵ^{-3}, ϵ^{-2}, and ϵ^{-1} parts of these diagrams involve much the same types of radial integrations as the ϵ^{-2}, ϵ^{-1}, and ϵ^0 parts, respectively, of the two-loop subdiagrams of class B. The principal differences between classes B and C are the following: First, the angular integrations are more complicated in class C and the radial and angular integrations cannot be performed in arbitrary order; and second, there is an enormous proliferation of the number of numerator terms in the class C diagrams.

There are three reasons for the large number of terms involved in computing these diagrams. First, the numerator traces are complicated, consisting of on the order of fifty different types of terms. Second, each of the numerator terms is a product of up to three direction cosines; use of the recursion relation (34) to reduce these cosines to Gegenbauer polynomials increases the number of terms by a factor of 2 for each direction cosine. Third, there are four momenta in the problem and therefore 4! regions of radial integration. Actually, power counting shows that only 12 of these regions contribute pole terms for diagrams C1 and C3 and 16 for diagram C2; symmetries reduce these numbers to 6 and 8, respectively. It is clearly not practical to evaluate the integrals term by term and region by region as was done with the diagrams of class B. The calculation was done region by region, integrating all terms simultaneously in each region using the algebraic-manipulation program SCHOONSCHIP.[41] (Problems with speed and memory space caused us to abandon an attempt to use MACSYMA for this phase of the calculation.)

We now discuss the problem, referred to above, concerning the order in which the radial and angular integrals are to be evaluated. Let us consider the "Benz" diagram of Fig. 4, i.e., the Feynman integral (51). There are five denominators to be expanded in Gegenbauer polynomials. Because the denominators do not involve $\hat{p}\cdot\hat{q}$, the angular integrations could, if one ignored the numerator, be performed in the order $\int d\hat{p}$ followed by $\int d\hat{k}$ or $\int d\hat{l}$ using Eqs. (39) and (36). Note that one would not be able to do the $\hat{k}$ or $\hat{l}$ integrations before the $\hat{p}$ integration because one would encounter integrals of three Gegenbauer polynomials such as

$$\int d\hat{k}\, C_{n_1}(\hat{k}\cdot\hat{l})C_{n_2}(\hat{k}\cdot\hat{p})C_{n_3}(\hat{k}\cdot\hat{q}) \tag{56}$$

for which there appears to exist no simple closed form. The numerator, however, certainly contains powers of $\hat{p}\cdot\hat{q}$. On expanding these powers in Gegenbauer polynomials, one would be faced with integrals such as (56) in the $\hat{p}$ as well as the

TABLE II. Values of the Feynman integrals corresponding to the diagrams of Fig. 3, and partial sums for Figs. 3(a)–3(d). To obtain the contribution to $D_B(Q)$ add the numbers in the last four columns multiplied by the factor at the head of the column, and then multiply by an overall factor of

$$\sum_i \epsilon_i^2 G_W \frac{\alpha_B}{\pi}\alpha_{cB}{}^2\left(\frac{\Omega_N}{\Omega_4}\frac{(2\pi)^4}{(2\pi)^N}\right)^3 Q^{-3\epsilon}.$$

Diagram	Group weight G_W	Coefficient of ϵ^{-3}	ϵ^{-2}	ϵ^{-1}	$\zeta(3)\,\epsilon^{-1}$
A3	$C_{2F}C_{2A}$	5/54	187/648	5335/7776	
B2		−5/54	−277/648	−11851/7776	5/6
B3		1/6	11/24	343/288	−1/6
C1		−1/6	−17/24	−727/288	5/3
(a)			−7/18	−469/216	7/3
A4	$C_{2F}{}^2$	−1/18	−25/216	−757/2592	
A5		−1/9	−11/54	−157/324	
A6		−1/18	−11/108	−83/324	
B4		1/3	37/36	1441/432	−2
C2		−1/9	−95/216	−3971/2592	1
(b)			1/6	37/48	−1
B5	$C_{2F}{}^2 - \frac{C_{2F}C_{2A}}{2}$	1/9	19/108	607/1296	
C3		−1/9	−49/108	−1465/1296	4/3
D			1/9	−19/216	−1/3
(c)			−1/6	−3/4	1
A7	$C_{2F}n_f$	−1/27	−35/324	−1007/3888	
B6		1/27	53/324	2267/3888	−1/3
(d)			1/18	35/108	−1/3
(a) $-\frac{1}{2}$(c)	$C_{2F}C_{2A}$		−11/36	−97/54	11/6
(b) + (c)	$C_{2F}{}^2$			1/48	

$\hat{k}$ and $\hat{l}$ variables. However, the residues of the poles are independent of the external momentum and hence really only involve the three loop momenta, which would lead one to suspect that there should be a way to avoid having to evaluate integrals such as (56). The solution to this problem is to evaluate the radial integrals before the angular integrals. It was found empirically that it was only necessary to evaluate one of the radial integrals, appropriately chosen, and then discard terms which could not contribute to the residues of the poles. This forced at least one of the indices n_1, n_2, n_3 in integrals such as (56) to zero. Since $C_0 = 1$, the angular integrals could then be evaluated.

Class D. Diagram D is the lone member of this class and the only diagram we have not computed. It is easily seen that this diagram is not planar when the external lines are joined together. It is also easy to convince oneself that at least one propagator must carry three momenta. There are two possible ways of dealing with this problem: (a) Since the pole part of the sum of all diagrams is independent of q, one should be able to set q to zero after differentiating twice with respect to q to get rid of an overall factor of q^2. One would then have to introduce an infrared cutoff such as a mass in one or more of the propagators in intermediate stages of the calculation. (b) In the spirit of the rest of this calculation one could continue to use the external momentum as an infrared cutoff as follows. The offending propagator is expanded to

$$\frac{1}{(\vec{p}-\vec{k}-\vec{q})^2} = \frac{1}{(\vec{p}-\vec{k})^2+q^2} + \frac{2(\vec{p}-\vec{k})\cdot\vec{q}}{[(\vec{p}-\vec{k})^2+q^2]^2} + \frac{4[(\vec{p}-\vec{k})\cdot\vec{q}]^2}{[(\vec{p}-\vec{k})^2+q^2]^3} + \cdots . \tag{57}$$

Power counting shows that the integral is infrared finite term by term, and that the expansion (57) can be terminated at the third term to obtain the pole parts of the diagram. One would then have to expand the denominators in (57) in Gegenbauer polynomials $C_n^{\lambda}(\hat{p}\cdot\hat{k})$. Such expansions are in principle straightforward to derive using Eqs. (41) and (42). The q^2 in (57) acts very much like a mass. In view of the existence of Rosner's well-known result from which the contribution of some of the QED diagrams can readily be obtained as explained in Sec. III A, we have not actually carried out this suggestion.

Table II lists our results for the pole parts of the three-loop diagrams of Fig. 3.

IV. CONCLUSIONS

We have presented an analytical calculation of the fourth-order QCD contributions to the process $e^+e^- \to$ hadrons. The calculation was done using a novel extension of the Gegenbauer-expansion technique to $4-\epsilon$ dimensions in momentum space.

The implications of this calculation for phenomenology are as follows. The parton model predicts scaling for processes such as $e^+e^- \to$ hadrons. Perturbative QCD corrections computed to lowest order in $\alpha_c(Q)$ predict logarithmic corrections to the parton-model result. More precisely, they predict the Q dependence of scaling violations. The next-to-leading-order QCD corrections then determine the scale Λ of the effective coupling constant and thus the overall magnitude of this Q dependence.

In order for the next-to-leading-order corrections to have any predictive content, one must compare two or more processes. This is simply because the dominant effect of these corrections is to determine Λ. Any one process can be chosen to serve as a measurement of Λ; one then obtains absolute predictions for every other process.

The coefficients in next-to-leading order are renormalization-prescription dependent. Since an $\alpha_c \approx 0.1$ rather marginally satisfies the requirements of a reliable expansion parameter,[6] one must be careful to renormalize the theory in a way which optimizes the convergence of the perturbation series. Strictly speaking, this can only be done if one could estimate higher uncalculated

TABLE III. Magnitude of perturbative massless-QCD corrections to the parton-model result $R = \sum_q \epsilon_q^2$ for typical values of $Q = \sqrt{s}$ and n_f. The running coupling constant has been computed using Eq. (58) with $\Lambda = 0.85$ GeV for the momentum-space subtraction (mom) scheme and $\Lambda = 0.5$ GeV for the $\overline{\text{MS}}$ scheme.

QCD effect	Renormalization scheme	$Q = 3$; $n_f = 3$	$Q = 5$; $n_f = 4$	$Q = 20$; $n_f = 5$	$Q = 40$; $n_f = 6$
α_c	mom	0.125	0.100	0.067	0.064
	$\overline{\text{MS}}$	0.089	0.079	0.058	0.057
$\alpha_c + K\alpha_c^2$	mom	0.098	0.084	0.061	0.059
	$\overline{\text{MS}}$	0.102	0.088	0.063	0.061

orders in perturbation theory. In practice, one can choose a definition of α_c which makes the calculated next-to-leading-order coefficients small in a number of processes.

The magnitude of the next-to-leading-order coefficient K in e^+e^- annihilation in a modified minimal-subtraction ($\overline{\text{MS}}$) scheme and in a momentum-space subtraction scheme are given in Eqs. (5) and (6), respectively. These schemes have been shown to give higher-order coefficients of reasonable size in other processes[42]; the fact that K_{mom} is small (e.g., $K_{\text{mom}} = -1.545$ for $n_f = 4$) supports the conjecture[17] that defining α_c by momentum-space subtraction will minimize higher-order corrections in general.

To obtain a prediction for the magnitude of higher-order correction terms, one must specify Λ, which determines α_c through the order in which we are interested via the formula

$$\alpha_c(Q) = \frac{1}{\beta_0 \ln(Q/\Lambda)} - \frac{\beta_1}{\beta_0^3} \frac{\ln\ln(Q^2/\Lambda^2)}{\ln^2(Q/\Lambda)} + O\left(\frac{1}{\ln^3(Q/\Lambda)}\right) \tag{58}$$

gotten by integrating Eq. (22), with the constant of integration being fixed by convention[10,17] such that (58) contains no additional term of the form const/$\ln^2(Q/\Lambda)$. At present, the best estimates of Λ come from deep-inelastic scattering data.[43] If one uses the $\overline{\text{MS}}$ scheme, one obtains a value of $\Lambda_{\overline{\text{MS}}} \cong 0.5$ GeV; momentum-space subtraction favors a larger value of $\Lambda_{\text{mom}} \cong 0.85$ GeV and hence a slightly larger coupling constant. In Table III we list values of $\alpha_c(Q)$ and $(\alpha_c + K\alpha_c^2)$ for typical values of Q and n_f. The sum of leading- and next-to-leading-order corrections is practically identical in the two schemes: The fact that Λ_{mom} is larger than $\Lambda_{\overline{\text{MS}}}$ is compensated for by the fact that K_{mom} is negative.

In conclusion, we note that it will be possible in the near future to use e^+e^- annihilation cross-section measurements to determine Λ as more accurate data become available from experiments at PETRA and PEP. The small size of the next-to-leading-order corrections (~15% relative to the leading order) indicates that the perturbative aspects of QCD predictions for this process are reliably under control in regions of Q^2 where mass and threshold effects are not important.

During the course of this calculation we learned that Dine and Sapirstein[44] have computed K numerically. Our results agree with theirs to within their stated computational errors on the final result as well as on transverse subsets of diagrams.[37,45] Our calculation was substantially complete when we became aware of an independent analytical calculation by a Russian group[46] using somewhat different techniques. These authors quote a final result which agrees with our Eq. (4).

ACKNOWLEDGMENTS

We are grateful to very many of our colleagues for discussions, advice and encouragement, in

TABLE IV. Values of the two-loop integrals I(numerator) defined in Eq. (B3). Since the denominator is symmetric in k_1 and k_2, I(numerator(k_1,k_2)) $= I$(numerator(k_2,k_1)).

num(k_1,k_2)	b_1	b_2	b_3
(a) $I(\text{num}(k_1,k_2)) = \frac{b_1}{\epsilon^2} + \frac{b_2}{\epsilon} + b_3$			
$(\vec{k}_1\cdot\vec{k}_2)(\vec{k}_1\cdot\vec{q})$	1/16	17/64	147/256
$(\vec{k}_1\cdot\vec{q})(\vec{k}_2\cdot\vec{q})$	0	1/16	9/64 + 3ζ(3)/8
$(\vec{k}_1\cdot\vec{k}_2)^2$	0	3/32	29/128
$(\vec{k}_1\cdot\vec{k}_2)q^2$	0	1/4	5/8
$k_1^2(\vec{k}_2\cdot\vec{q})$	1/4	7/16	49/64
$k_1^2 k_2^2$	0	0	0
$k_1^2 q^2$	1/2	3/4	5/4
$(\vec{k}_1\cdot\vec{q})^2$	1/8	7/32	49/128 + 3ζ(3)/8
(b) $I(\text{num}(k_1,k_2)\lvert\vec{k}_1-\vec{k}_2\rvert^{-\epsilon}) = q^{-\epsilon}\left(\frac{b_1}{\epsilon^2} + \frac{b_2}{\epsilon} + b_3\right)$			
$(\vec{k}_1\cdot\vec{k}_2)(\vec{k}_1\cdot\vec{q})$	1/48	31/192	425/768
$(\vec{k}_1\cdot\vec{q})(\vec{k}_2\cdot\vec{q})$	0	1/24	7/48 + 3ζ(3)/8
$(\vec{k}_1\cdot\vec{k}_2)^2$	0	1/16	11/48
$(\vec{k}_1\cdot\vec{k}_2)q^2$	0	1/6	2/3
$k_1^2(\vec{k}_2\cdot\vec{q})$	1/12	1/4	31/48
$k_1^2 k_2^2$	0	0	0
$k_1^2 q^2$	1/6	5/12	1
$(\vec{k}_1\cdot\vec{q})^2$	1/24	11/96	113/384 + 3ζ(3)/8
(c) $I(\text{num}(k_1,k_2)k_1^{-\epsilon}) = q^{-\epsilon}\left(\frac{b_1}{\epsilon^2} + \frac{b_2}{\epsilon} + b_3\right)$			
$(\vec{k}_1\cdot\vec{k}_2)(\vec{k}_1\cdot\vec{q})$	1/48	31/192	123/256
$(\vec{k}_1\cdot\vec{k}_2)(\vec{k}_2\cdot\vec{q})$	1/24	3/16	25/48
$(\vec{k}_1\cdot\vec{q})(\vec{k}_2\cdot\vec{q})$	0	1/24	1/8 + 3ζ(3)/8
$(\vec{k}_1\cdot\vec{k}_2)^2$	0	1/24	5/48
$(\vec{k}_1\cdot\vec{k}_2)q^2$	0	1/6	7/12
$k_1^2(\vec{k}_2\cdot\vec{q})$	1/12	1/4	29/48
$k_2^2(\vec{k}_1\cdot\vec{q})$	1/6	1/3	17/24
$k_1^2 k_2^2$	0	−1/12	−7/24
$k_1^2 q^2$	1/6	5/12	1
$k_2^2 q^2$	1/3	2/3	17/12
$(\vec{k}_1\cdot\vec{q})^2$	1/24	11/96	113/384 + 3ζ(3)/8
$(\vec{k}_2\cdot\vec{q})^2$	1/12	3/16	5/12 + 3ζ(3)/8

particular to S. Brodsky, N. Christ, R. Dashen, W. Frazer, H. Georgi, D. Gross, N. Kroll, J. Richardson, D. Sivers, and D. Wong. We thank the Mathlab Group at the MIT Laboratory for Computer Science for the use of MACSYMA, and G. Masek, W. Vernon, and co-workers for computer advice. We would like to thank R. Brenner for the use of his MACSYMA program DIAGEVAL[47] to do some of the traces. R. J. G. would like to thank the theory groups at Fermilab, Los Alamos, and SLAC for their kind hospitality and computer support during the summer of 1979, and M. Dine for a helpful remark concerning a SCHOONSCHIP trace routine. This work was supported in part by the United States Department of Energy.

APPENDIX A

In this appendix we will derive Eqs. (45) and (46) and obtain an expansion for $[(\vec{k}-\vec{l})^2]^{-1-\epsilon/2}$.

If one substitutes the expansion of the hypergeometric function given in Eq. (44) in Eq. (43), one obtains by straightforward differentiation

$$\left.\frac{d}{d\epsilon}G_n\right|_{\epsilon=0} = -\frac{1}{2}\left.\frac{d}{d\lambda}G_n\right|_{\lambda=1}$$
$$= \psi(n+2) - \frac{1}{2(n+1)} - \ln(1-x)$$
$$-\left(\frac{1-x}{2}\right)\sum_{m=0}^{\infty} x^m[\psi(m+1)+\psi(n+m+2)]. \tag{A1}$$

Here $\psi(x) \equiv (d/dx)\ln\Gamma(x)$. The last term can be rearranged as follows:

$$(1-x)\sum_{m=0}^{\infty} x^m[\psi(m+1)+\psi(n+m+2)]$$
$$= \psi(1)+\psi(n+2)+\sum_{m=1}^{\infty} x^m[\psi(m+1)-\psi(m)$$
$$+\psi(n+m+2)-\psi(n+m+1)]. \tag{A2}$$

Equation (45) then follows if one uses the formula[48]

$$\psi(n) = \psi(1) + \sum_{j=1}^{n-1}\frac{1}{j}, \quad n \geq 2 \tag{A3}$$

to simplify (A2) and (A1).

The asymptotic form (46) for $G_n(x)$ in the limit $x \to 1$ is obtained most easily by using the linear transformation formula[48]

$${}_2F_1(a,b;c;x)$$
$$= \frac{\Gamma(c)\Gamma(c-a-b)}{\Gamma(c-a)\Gamma(c-b)}\,{}_2F_1(a,b;a+b-c+1;1-x)$$
$$+(1-x)^{c-a-b}\frac{\Gamma(c)\Gamma(a+b-c)}{\Gamma(a)\Gamma(b)}$$
$$\times {}_2F_1(c-a,c-b;c-a-b+1;1-x) \tag{A4}$$

which is valid for $|\arg(1-x)| < \pi$, in conjunction with the series expansion (44). It is useful to keep in mind that the expansion (44) is absolutely convergent for $|x| < 1$.

We shall now derive an expansion in Gegenbauer polynomials for

$$\left(\frac{1}{(\vec{k}-\vec{l})^2}\right)^{\mu} = \left(\frac{1}{(kl)_>}\right)^{\mu}\left(\frac{1}{1-2zt+z^2}\right)^{\mu}, \tag{A5}$$

where $z \equiv z_{kl}$ and $t \equiv \hat{k}\cdot\hat{l}$ [see Eq. (43)]. Let

$$(1-2zt+z^2)^{-\mu} = \sum_{n=0}^{\infty} z^n H_n(z^2;\mu)C_n^{\lambda}(t). \tag{A6}$$

That H_n is a function of z^2 follows from the fact that $C_n^{\lambda}(-t) = (-)^n C_n^{\lambda}(t)$. We obviously have

$$H_n(z^2;1) = G_n(z^2), \tag{A7}$$

and using the fact that

$$(1-2zt+z^2)^{-\lambda} = \sum_{n=0}^{\infty} z^n C_n^{\lambda}(t) \tag{A8}$$

is a generating function for the Gegenbauer polynomials,[34] we have

$$H_n(z^2;\lambda) = 1. \tag{A9}$$

Use of Rodrigues's formula[34]

$$C_n^{\lambda}(t) = (-)^n\frac{2^n}{n!}\frac{\Gamma(n+2\lambda)\Gamma(n+\lambda)}{\Gamma(\lambda)\Gamma(2n+2\lambda)}(1-t^2)^{1/2-\lambda}\frac{d^n}{dt^n}(1-t^2)^{n+\lambda-1/2} \tag{A10}$$

and the orthogonality relation (36), yields the following integral representation for H_n:

$$H_n(z^2;\mu) = \frac{n!(n+\lambda)[\Gamma(\lambda)]^2}{z^n\pi 2^{1-2\lambda}\Gamma(n+2\lambda)}\int_{-1}^{+1} dt\,\frac{(1-t^2)^{\lambda-1/2}C_n^{\lambda}(t)}{(1-2zt+z^2)^{\mu}}$$
$$= \frac{2}{\pi}\,2^{2n+2\lambda-1}\frac{\Gamma(\lambda)\Gamma(n+\lambda+1)\Gamma(\mu+n)}{\Gamma(2n+2\lambda)\Gamma(\mu)}\int_{-1}^{+1} dt\,\frac{(1-t^2)^{n+\lambda-1/2}}{(1-2zt+z^2)^{\mu+n}}. \tag{A11}$$

Using (A11), it is simple to show that

$$H_n(0;\mu)=\frac{\Gamma(\lambda)}{\Gamma(\mu)}\frac{\Gamma(\mu+n)}{\Gamma(\lambda+n)},$$
$$\frac{d}{dz^2}H_n(z^2;\mu)\Big|_{z=0}=\left(\frac{\mu-\lambda}{n+1+\lambda}\right)\frac{\Gamma(\lambda)}{\Gamma(\mu)}\frac{\Gamma(\mu+n+1)}{\Gamma(\lambda+n)}. \tag{A12}$$

Now let us assume that $\mu-\lambda=O(\epsilon)$ and expand the first equality of (A11) about $\mu=\lambda$:

$$H_n(z^2;\mu)=1+(\lambda-\mu)\frac{2}{z^n\pi}\int_{-1}^{+1}dt\,\frac{(1-t^2)^{1/2}C_n^1(t)\ln(1-2zt+z^2)}{(1-2zt+z^2)}+O(\epsilon^2). \tag{A13}$$

We have made use of (A9). Upon evaluating (A13) with $\mu=1$ and $\mu=1+\epsilon/2$ and comparing the resulting expressions through order ϵ, we obtain

$$\frac{d}{d\epsilon}H_n(z^2;1+\epsilon/2)\Big|_{\epsilon=0}=2\frac{d}{d\epsilon}G_n(z^2)\Big|_{\epsilon=0}. \tag{A14}$$

The formulas (A12) and (A14) suffice to deal with the class B diagrams B2 and B6 as discussed in the text.

APPENDIX B: TWO-LOOP INTEGRALS

Class A and B diagrams are A1–A7 and B1–B6 (see Figs. 1–3). Diagrams such as B3 are computed by first calculating the two-loop insertions on the quark line and then making the insertion in the one-loop diagram. The two-loop self-energy diagram (i.e., the quark insertion) depends on the (internal) momentum k as $k^{-2\epsilon}$ so the one-loop diagram with insertion simply requires calculating $I_1(2)$ where (all momenta Euclidean)

$$I_1(a)=\int d_Nk\,\frac{\mathrm{Tr}[\gamma^\mu(\not k-\not q)\gamma_\mu\not k]k^{-a\epsilon}}{k^2(\vec k-\vec q)^2}. \tag{B1}$$

The trace in (B1) must, of course, be computed in $N=(4-\epsilon)$ dimensions. The integral in (B1) is easily evaluated through $O(\epsilon)$ as described in the text [see Eq. (47) and the subsequent discussion]. The result is

$$I_1(a)=q^{2-(1+a)\epsilon}\frac{\Omega_N}{a+1}\times[4/\epsilon+3a+(7a^2+10a+4)\epsilon/4+O(\epsilon^2)]. \tag{B2}$$

In a similar way, diagram B4 (for instance) can be computed by calculating the one-loop fermion insertion in the two-loop diagram. Since the resulting three-loop graph need only be computed through $O(1/\epsilon)$, the two-loop diagram need only be expanded through $O(\epsilon^0)$. The nontrivial integrals to be evaluated are

$$I(\text{numerator})\equiv\frac{q^{2\epsilon}}{\Omega_N{}^2}\int d_N\vec k_1 d_N\vec k_2\times\frac{\text{numerator}}{k_1{}^2k_2{}^2(\vec k_1-\vec k_2)^2(\vec k_1-\vec q)^2(\vec k_2-\vec q)^2}.$$

These integrals are tabulated in Table IV.

*Present address: Argonne National Laboratory, Argonne, Illinois 60439.

[1]J. Bjorken, Phys. Rev. 148, 1467 (1966); V. N. Gribov, B. L. Ioffe, and I. Ya. Pomeranchuk, Phys. Lett. 24B, 554 (1967).

[2]R. P. Feynman, *Photon Hadron Interactions* (Benjamin, Reading, Mass., 1972); J. D. Bjorken and E. Paschos, Phys. Rev. 185, 1975 (1969); S. D. Drell, D. Levy, and T.-M. Yan, Phys. Rev. 187, 2159 (1969).

[3]N. Cabbibo, G. Parisi, and M. Testa, Nuovo Cimento Lett. 4, 35 (1970). The extension to three colors was given by W. A. Bardeen, H. Fritzsch, and M. Gell-Mann, in *Scale and Conformal Symmetry in Hadron Physics*, edited by R. Gatto (Wiley, New York, 1973).

[4]D. J. Gross and F. Wilczek, Phys. Rev. Lett. 30, 1343 (1973); H. D. Politzer, *ibid.* 30, 1346 (1973); G. 't Hooft (unpublished).

[5]See e.g., D. J. Gross and F. Wilczek, Phys. Rev. D 8, 3633 (1973); H. D. Politzer, Phys. Rep. 14C, 129 (1974).

[6]It is hoped that the use of α_c (c stands for color or chromodynamic), instead of conventional $\alpha_s=g^2/4\pi=\pi\alpha_c$, in this paper will lead to no confusion. It has been argued [see, e.g., D. J. Gross in *Methods in Field Theory*, edited by R. Balian and J. Zinn-Justin (North-Holland, Amsterdam, 1976), p. 210] that α_c, and not α_s, is the natural expansion parameter in QCD perturbation theory. From a practical point of view, the use of α_c eliminates an unnecessary and messy proliferation of factors of π in various equations in this paper.

[7]See, e.g., the review talk by G. J. Feldman, in *Proceedings of the 19th International Conference on High Energy Physics, Tokyo, 1978*, edited by S. Homma, M. Kawaguchi, and H. Miyazawa (Phys. Soc. of Japan, Tokyo, 1979).

[8]T. Appelquist and H. Georgi, Phys. Rev. D 8, 4000 (1973); A. Zee, *ibid.* 8, 4038 (1973).

[9]M. Bacé, Phys. Lett. 78B, 132 (1978).

[10]E. G. Floratos, D. A. Ross, and C. T. Sachrajda, Nucl. Phys. B129, 66 (1977); B139, 545(E) (1978); W. A. Bardeen, A. Buras, D. W. Duke, and T. Muta,

Phys. Rev. D 18, 3998 (1978).
[11]W. A. Bardeen and A. Buras, Phys. Rev. D 20, 166 (1979).
[12]G. Altarelli, R. K. Ellis, and G. Martinelli, Nucl. Phys. B143, 521 (1978); B146, 544(E) (1978); Nucl. Phys. B157, 461 (1979); J. Kubar-André and F. E. Paige, Phys. Rev. D 19, 221 (1979); K. Harada, T. Kaneko, and N. Sakai, Nucl. Phys. B155, 169 (1979); A. P. Contogouris and J. Kripfganz, Phys. Lett. 84B, 473 (1979); Phys. Rev. D 19, 2207 (1979); J. Abad and B. Humpert, Phys. Lett. 83B, 371 (1979); 80B, 286 (1979).
[13]R. Barbieri, E. D'Emilio, G. Curci, and E. Remiddi, Nucl. Phys. B154, 535 (1979).
[14]G. 't Hooft, Nucl. Phys. B61, 455 (1973). Renormalization is implemented by subtracting only the pole parts of Green's functions regularized by the dimensional continuation method of G. 't Hooft and M. Veltman, Nucl. Phys. B44, 189 (1972); C. G. Bollini and J. J. Giambiagi, Phys. Lett. 40B, 566 (1972); J. F. Ashmore, Nuovo Cimento Lett. 4, 289 (1972).
[15]The reader is cautioned that some authors include an additional factor of 2 or $1/8\pi^2$ in what they call β_0. Our definition of β_0 follows that of Gross in Ref. 6.
[16]In practice, this factor arises from a combination of the essentially arbitrary formula $\Omega_N = 2\pi^{N/2}/\Gamma(N/2)$ used to continue the volume of the unit sphere in integer N dimensions to arbitrary N, and the conventional but equally arbitrary replacement of the usual $(2\pi)^{-4}$ by $(2\pi)^{-N}$ in the Feynman rules when one uses dimensional regularization. Every loop integration then contributes a factor

$$\frac{\Omega_N}{(2\pi)^N} = 1/8\pi^2\left[1+\frac{\epsilon}{2}\left(\ln(4\pi)+1-\gamma_E\right)+O(\epsilon^2)\right].$$

In fact, every such factor is multiplied by $g_B{}^2$, where g_B is the appropriate bare coupling constant which has dimensions $(\text{mass})^{\epsilon/2}$. The $\overline{\text{MS}}$ scheme corresponds to the rescaling

$$g_B{}^2 \to g_B{}^2\{1-(\epsilon/2)[\ln(4\pi)-\gamma_E]+O(\epsilon^2)\}.$$

One is tempted to define an MS′ scheme in which the coupling is rescaled as follows:

$$g_B{}^2 \to g_B{}^2 \frac{\Omega_4}{\Omega_N}\frac{(2\pi)^N}{(2\pi)^4},$$

i.e., one forces $\Omega_N/(2\pi)^N$ to its four-dimensional value in continuing away from $N=4$. This corresponds to absorbing a factor of $[\ln(4\pi)-\gamma_E+1]$ compared with $[\ln(4\pi)-\gamma_E]$ in the $\overline{\text{MS}}$ scheme. Rather surprisingly the MS′ scheme yields a definition of α_c that is practically identical with the momentum-space subtraction schemes.
[17]W. Celmaster and R. J. Gonsalves, Phys. Rev. Lett. 42, 1435 (1979); Phys. Rev. D 20, 1420 (1979).
[18]For a similar proposal, see R. Barbieri, L. Caneschi, G. Curci, and E. d'Emilio, Phys. Lett. 81B, 207 (1979).
[19]The result given by us in the second paper of Ref. 17 was obtained by defining the vertex renormalization constant $Z_{1F}{}^{-1}$ as the coefficient of γ_μ after decomposing the one-particle irreducible quark-gluon three-point function using the set of tensors $\{\gamma_\mu, \not{p}p_\mu, \not{p}r_\mu, \gamma_5\gamma^\nu\epsilon_{\mu\nu\alpha\beta}p_\alpha r_\beta\}$. The various quantities are defined in Fig. 3(c) of this reference. We thank T. Goldman for pointing out that it is necessary to specify this set to unambiguously determine the finite part of Z_{1F}.
[20]See e.g., L. Lewin, *Dilogarithms and Associated Functions* (Macdonald, London, 1958). Clausen's function attains its maximum value at $\theta=\pi/3$ where it can be related to a dilogarithm:

$$\mathrm{Cl}_2\left(\frac{\pi}{3}\right)=\frac{\pi^2}{4}+\mathrm{Li}(-2)$$
$$=-\frac{\sqrt{3}}{2}\int_0^1 dx\,\frac{\ln x}{1-x+x^2}\equiv\frac{\sqrt{3}}{4}\mathcal{G};$$

the results of Ref. 17 were expressed in terms of the integral $\mathcal{G}$.
[21]See e.g., J. L. Rosner, Ann. Phys. (N.Y.) 44, 11 (1967); E. de Raphael and J. L. Rosner, *ibid.* 82, 369 (1974); M. J. Levine and R. Roskies, Phys. Rev. D 9, 421 (1974).
[22]S. L. Adler, Phys. Rev. D 10, 3714 (1974).
[23]E. C. Poggio, H. R. Quinn, and S. Weinberg, Phys. Rev. D 13, 1958 (1976); see also R. Shankar, *ibid.* 15, 755 (1977).
[24]T. Appelquist and J. Carazzone, Phys. Rev. D 11, 2856 (1975).
[25]A De Rújula and H. Georgi, Phys. Rev. D 13, 1296 (1976); R. G. Moorhouse, M. R. Pennington, and G. G. Ross, Nucl. Phys. B124, 285 (1977).
[26]W. Caswell, Phys. Rev. Lett. 33, 244 (1974); D. R. T. Jones, Nucl. Phys. B75, 531 (1974).
[27]Moorhouse, Pennington, and Ross (Ref. 25) examine the validity of this assumption.
[28]J. Schwinger, Phys. Rev. 74, 1439 (1948); see also W. Pauli and F. Villars, Rev. Mod. Phys. 21, 434 (1949).
[29]R. Jost and J. M. Luttinger, Helv. Phys. Acta 23, 201 (1950).
[30]G. Källén and A. Sabry, Dan. Mat. Fys. Medd. 29, No. 17 (1955). In QED, $d_{2,0}=-\frac{5}{24}+\zeta(3)$, see C. R. Hagen and M. A. Samuel, Phys. Rev. Lett. 20, 1405 (1968), B. E. Lautrup and E. de Raphael, Phys. Rev. 174, 1835 (1968).
[31]J. L. Rosner, Phys. Rev. Lett. 17, 1190 (1966).
[32]Rosner actually did the calculation for zero electron mass, so there is no question of finite mass-renormalization effects in using his result in our calculation. It can be shown that a finite-mass counter term insertion renders the vacuum-polarization diagram in Fig. 1 and sum of diagrams in Fig. 2 finite. The proof of a generalization of this result to all orders can be found in K. Johnson, R. Willey, and M. Baker, Phys. Rev. 163, 1699 (1967).
[33]A. A. Vladimirov, Theor. Math. Phys. 36, 732 (1979); K. G. Chetyrkin and F. V. Tkachov, Moscow Report No. II-0118, 1979 (unpublished); T. Curtright, U. of Chicago Report No. EFI-79/36, 1979 (unpublished).
[34]A rigorous discussion of the properties of these polynomials can be found in G. Szegö, *Orthogonal Polynomials* (Amer. Math. Soc. Colloq. Pub. 23, 1959). For a very useful compendium of formulas see W. Magnus, F. Oberhettinger, and R. P. Soni, *Formulas and Theorems for the Special Functions of Mathematical Physics* (Springer, Berlin, 1966).

[35]L. Durand, P. M. Fishbane, and L. M. Simmons, Jr., J. Math. Phys. 17, 1933 (1976).

[36]G. Leibbrandt, Rev. Mod. Phys. 47, 849 (1975). See also e.g., W. J. Marciano and A. Sirlin, Nucl. Phys. B88, 86 (1975); P. Cvitanović, *ibid.* B130, 114 (1977).

[37]Each of the diagrams we compute is not separately transverse. In addition to the sum of all diagrams, there are various subsets which are transverse by themselves. These are sets invariant under the operation of attaching one of the external photon lines at all possible positions on the quark loop: See, e.g., J. D. Bjorken and S. D. Drell, *Relativistic Quantum Fields* (McGraw-Hill, New York 1965), p. 199. Such sets are (A2+B1), (A3+B2), (B3+C1), (A4+$\frac{1}{2}$B4+C2), (A5+A6+$\frac{1}{2}$ B4), (B5+C3+D), and (A7+B6) in Figs. 2 and 3.

[38]The criterion of planarity is spelled out in greater detail by Levine and Roskies (Ref. 21).

[39]We remind the reader that we are interested in the finite part of the diagrams in Fig. 2 and the pole parts of those in Fig. 3.

[40]The QED β function turns out to be free of $\zeta(3)$ as well: See de Raphael and Rosner, Ref. 21, who discuss the cancellation of factors of $\zeta(3)$ in QED. It is a curious fact that this transcendental number occurs precisely in the form $\beta_0\zeta(3)$ in our final results. (See, e.g., Eq. (4) where it is naturally associated with the factor $[\ln(4\pi)-\gamma_E]$.)

[41]M. Veltman, CERN report, 1967 (unpublished); H. Strubbe, Comput. Phys. Commun. 8, 1 (1974).

[42]See e.g., Refs. 10, 11, and 17. It might be pointed out that the calculation of the next-to-leading-order perturbative corrections to the decay rate of pseudoscalar quarkonium by Barbieri *et al.*, Ref. 13, favor the momentum-space subtraction scheme over the $\overline{\text{MS}}$ scheme.

[43]A. J. Buras [Rev. Mod. Phys. 52, 199 (1980)] has a comprehensive review of deep-inelastic processes and, in particular, the extraction of Λ as defined by various renormalization schemes from the data.

[44]M. Dine and J. Sapirstein, Phys. Rev. Lett. 43, 668 (1979).

[45]W. Celmaster and R. J. Gonsalves, Phys. Rev. Lett. 44, 560 (1980).

[46]K. G. Chetyrkin, A. L. Kataev, and F. V. Tkachov, Phys. Lett. 85B, 277 (1979).

[47]R. Brenner, Caltech Report No. CALT-68-702, 1979 (unpublished).

[48]*Handbook of Mathematical Functions*, edited by M. Abramowitz and I. A. Stegun, Natl. Bur. Stand. Applied Mathematics Series, No. 55 (U.S. GPO, Washington, D.C., 1964).